



Cite this: *CrystEngComm*, 2016, 18, 8439

Recombinant perlucin derivatives influence the nucleation of calcium carbonate†

Eva Weber,^a Ingrid M. Weiss,^{ab} Helmut Cölfen^c and Matthias Kellermeier^{*d}

Proteins are known to play various key roles in the formation of complex inorganic solids during natural biomineralisation processes. However, in most cases our understanding of the actual underlying mechanisms is rather limited. One interesting example is perlucin, a protein involved in the formation of nacre, where it is believed to promote the crystallisation of calcium carbonate. In the present work, we have used potentiometric titration assays to systematically investigate the influence of recombinant GFP-labeled perlucin derivatives on the early stages of CaCO₃ formation. Our results indicate that different parts of the protein can impact nucleation in distinct ways and act in either a retarding or promoting fashion. The most important finding is that full-length GFP-perlucin changes the nature of the initially precipitated phase and seems to favour the direct formation of crystalline polymorphs over nucleation of ACC and subsequent phase transformation, as observed in reference experiments without protein. This confirms the supposed role of perlucin in nacre biomineralisation and may rely on specific interactions between the protein and the crystal lattice of the emerging mineral phase.

Received 28th August 2016,
Accepted 11th October 2016

DOI: 10.1039/c6ce01878e

www.rsc.org/crystengcomm

Introduction

Strategies of how organisms control the mineralisation of inorganic matter throughout their tissues are a subject of continuous interest and debate.^{1,2} Recently, proteomic studies revealed certain “toolkits of biomineralisation”, such as macromolecules isolated from the nacreous and prismatic layers of *Pinctada* species³ or from the skeletal organic matrix of the stony coral *Stylophora*.⁴ These approaches clearly demonstrate the importance of a concerted interplay between multiple organic constituents in biomineralisation processes and it remains an open question which minimal requirements are needed in order to achieve controlled crystallisation in such environments.

Regarding the complexity of these systems, it is evident that distinct roles of individual macromolecules and functional protein domains have to be evaluated in simplified experiments first. Standardised and highly sensitive

mineralisation assays with biochemically well characterised proteins offer a unique approach to gain fundamental insight into the function of proteins and their influence on different species occurring in the course of the process.^{5,6} For calcium carbonate (one of the most important biominerals), potentiometric titrations have proven to be a powerful technique to monitor in particular the very early stages of crystallisation⁷ and to classify additives with respect to their various possible effects.⁸ This methodology has been successfully applied to examine the influence of single amino acids,⁹ artificial peptides,¹⁰ carbohydrates,¹¹ as well as synthetic polymers.¹² However, similar comprehensive studies on actual biomineralisation proteins are rare.^{13–18}

Against this background we decided to study the role of perlucin during the early stages of CaCO₃ formation. Perlucin is a native protein produced by various mollusc species with different shell types and can be extracted for example from the mother-of-pearl layer of *Haliotis laevigata*.^{19,20} The C-terminal sequences of perlucin vary in the length of the repetitive elements, containing up to nine times “SLHANLQQRD” in a 240 amino acid precursor protein.^{21,22} Both native²³ and recombinant perlucin^{24–26} were shown to affect the crystallisation of calcium carbonate in previous *in vitro* assays and hence this protein is an interesting candidate for further in-depth studies of CaCO₃ nucleation and early growth behaviour. In view of the fact that perlucin has C-type lectin properties, various types of carbohydrates including chitin derivatives are likely candidates for mediating responsive perlucin interactions *in vivo*.

^a INM – Leibniz Institute for New Materials, Campus D2.2, D-66123 Saarbrücken, Germany

^b Biomaterials and Biomolecular Systems, University of Stuttgart, Pfaffenwaldring 57, D-70569 Stuttgart, Germany

^c Physical Chemistry, University of Konstanz, Universitätsstrasse 10, D-78464 Konstanz, Germany

^d Material Physics, BASF SE, GMC/O – B007, Carl-Bosch-Strasse 38, D-67056 Ludwigshafen, Germany. E-mail: matthias.kellermeier@basf.com;

Fax: +49 621 66 43388; Tel: +49 621 60 43388

† Electronic supplementary information (ESI) available: Additional figures (Fig. S1–S5) and experimental details. See DOI: 10.1039/c6ce01878e



It is known that recombinant perlucin tends to be insoluble and needs to be purified *via* denaturation/renaturation processes,²⁷ or modified for its native purification.^{24,28} The highly soluble green fluorescent protein (GFP) turned out to drastically increase the solubility of perlucin when expressed as a fusion protein (GFP-perlucin), thereby facilitating its accessibility for downstream analysis. With respect to calcium carbonate formation, GFP was found to act as an inhibitor while the influence of the perlucin part in the resulting chimeric fusion protein has not been addressed in detail so far.²⁸ Therefore, we have purified individual proteins by size-exclusion chromatography (SEC) and then investigated their effect on the formation of calcium carbonate in a controlled titration experiment at constant pH.

Results and discussion

GFP and the fusion protein GFP-perlucin were extracted from *E. coli*, purified and characterised biochemically as described in previous studies (see the ESI† for experimental details).^{25,28} In SEC, GFP-perlucin elutes in three distinct peak fractions (see Fig. S1 and S2 in the ESI†): fraction 1 (P1) contains predominantly the full-length protein, along with small amounts of a truncated version of the protein (see the Supplementary discussion in the ESI† for more information on the sequence of the used proteins). The latter species represents the main component found in peak fractions 2 and 3 (P2 and P3). Therefore, P2 and P3 were combined in one sample (P2–3). The as-obtained full-length GFP-perlucin (P1), truncated GFP-perlucin (P2–3), and GFP alone were subsequently transferred into 10 mM NaHCO₃/Na₂CO₃ buffer at pH 9.00 and an effective individual protein concentration of 0.01 mg mL⁻¹. It is worth noting that GFP-perlucin tends to agglomerate and adsorb on surfaces, leading to a greater or lesser uncertainty regarding the final concentration in the reaction beaker.

In order to induce CaCO₃ precipitation, dilute calcium chloride solution was titrated continuously into the protein-containing carbonate buffer until nucleation occurred and crystals were formed. During CaCl₂ addition, the pH of the buffer was kept constant at 9.00 by automated counter-titration of NaOH, while the free concentration of calcium ions was monitored by an ion-selective electrode (ISE).⁷ This gave time-dependent profiles as those shown in Fig. 1, represented either as detected free molar amounts of Ca²⁺ ($n_{\text{free}}(\text{Ca}^{2+})$, Fig. 1a) or the corresponding concentration products of free calcium and carbonate ions ($c_{\text{free}}(\text{Ca}^{2+}) \cdot c_{\text{free}}(\text{CO}_3^{2-})$, Fig. 1b). In general, the amount of free Ca²⁺ first increases linearly upon CaCl₂ addition, however at a rate that is distinctly lower than expected based on the known dosed volumes (indicated as dashed grey line in Fig. 1a). The difference between added and detected calcium is due to binding of Ca²⁺ in ion pairs and/or larger ion clusters during the pre-nucleation stage, as described in detail elsewhere.^{7,29,30} At some critical point, the calcium concentration reaches a maximum and nucleation of a second phase takes place. In the

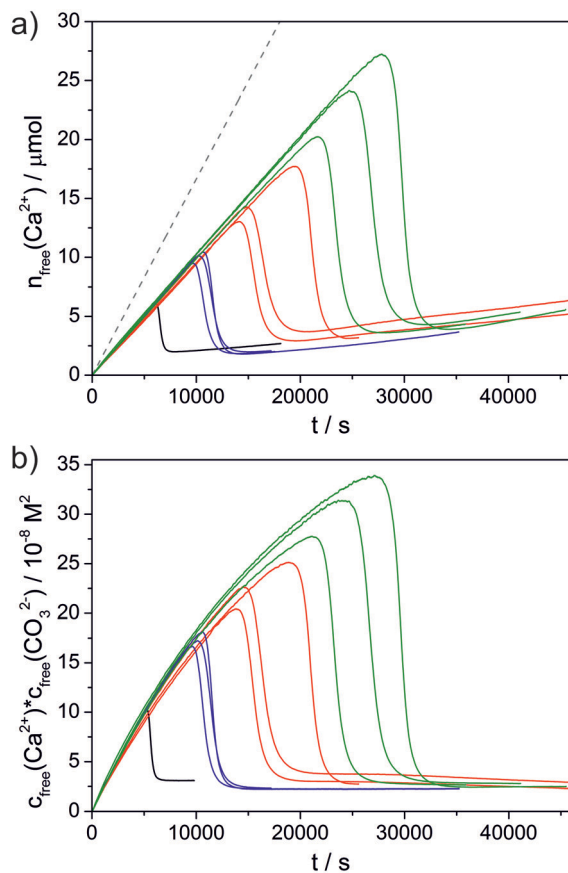


Fig. 1 Results of pH-constant titration experiments in 10 mM NaHCO₃/Na₂CO₃ buffer (pH 9.00) containing 0.01 mg mL⁻¹ of GFP (red), P1 (blue), or P2–3 (green), as compared to the reference experiment in the absence of any additives (black). For each protein, three independent measurements are shown. a) Time-dependent development of the amount of free Ca²⁺ traced upon continuous addition of 10 mM CaCl₂ into the buffer at a rate of 0.01 mL min⁻¹. The dashed grey line represents the dosed amount. b) Corresponding free ion products, calculated under the assumption that Ca²⁺ and CO₃²⁻ bind in equimolar ratios in both the pre- and post-nucleation stage (which is confirmed in all cases by the volumes of NaOH required to keep the pH of the buffer constant).

following, the amount of free Ca²⁺ decreases as the nucleated particles grow (and/or transform) and eventually levels off at a plateau, where the corresponding ion product indicates the solubility of the formed crystalline or amorphous phase.⁷

Additives can affect the progression of the titration profiles in various ways, as already shown in a number of previous studies.^{7–18} Here we focus on three distinct aspects: i) the equilibrium of ion association prior to nucleation (as reflected in the slope of the curve during the pre-nucleation stage); ii) the effect on the nucleation process itself (given by the position of the maximum); and iii) the nature of the solid phase present in the early post-nucleation regime (characterised by the solubility product mentioned above). The influence of the three studied proteins is summarised as bar plots in Fig. 2 and 3.

Regarding the formation of ion pairs and clusters in solution before nucleation (Fig. 2a), all three proteins seem to



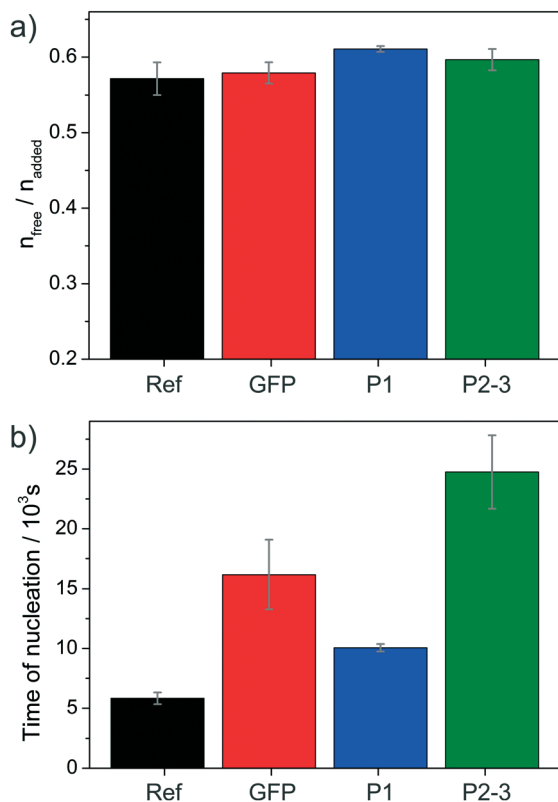


Fig. 2 Effect of the studied proteins on a) the pre-nucleation slope (given by the averaged ratio of the free and dosed amounts of Ca^{2+} before nucleation) and b) the time of nucleation (as determined from the maximum of the curves shown in Fig. 1a), both compared to the reference experiment without added protein (black). Values represent averages of at least three independent repetitions with corresponding standard deviations.

have a slight destabilising impact since more free Ca^{2+} ions are detected in equilibrium with the bound ones relative to the reference experiment without added proteins. However, the observed effects are generally small compared to other additives¹¹ and statistically significant only for the full-length GFP-perluciferin fusion protein (P1).

By contrast, much more pronounced influence is seen with respect to the time of nucleation (Fig. 2b), where all three proteins show distinct inhibiting power. Compared to the reference, nucleation is delayed by factors of 1.76, 2.84 and 4.34 in the presence of P1, GFP and P2–3, respectively. The fact that GFP inhibits CaCO_3 formation from solution is in line with previous observations.²⁸ On the other hand, the behaviour of the two fusion proteins is interesting, especially when considering that both carry a GFP residue as well. For the full-length protein P1, we find that the inhibitory effect of GFP is partly reversed, *i.e.* nucleation occurs earlier than with GFP alone. This suggests that some domains in the protein promote nucleation of calcium carbonate and thus compete with the delaying influence of GFP (and other domains). In turn, the truncated protein variant P2–3 shows very strong inhibition of nucleation, indicating that the structural domains removed upon truncation were those that actually activated

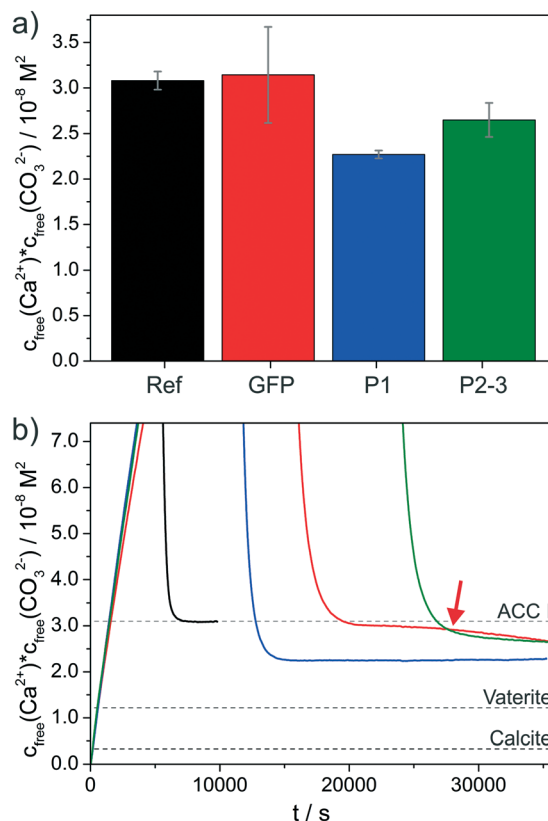


Fig. 3 Influence of the proteins on the solubility of the initially precipitated phase. a) Bar plots of the average free ion products observed directly after nucleation (as determined from the plateaus reached subsequent to the sharp decrease of $c_{\text{free}}(\text{Ca}^{2+}) \cdot c_{\text{free}}(\text{CO}_3^{2-})$ in Fig. 1b). b) Zoom into the early post-nucleation stage, evidencing differences in solubility induced by the distinct proteins (color code as in Fig. 1). Dashed lines indicate solubility products reported for an ACC phase with proto-calcitic short-range order,²⁹ as well as for the two anhydrous crystalline polymorphs vaterite and calcite in their bulk form.³¹ Note that the relatively large error bar for GFP in (a) is due to the fact that the free ion product still changes after nucleation (as indicated by the red arrow), thus leading to a larger variation of values at the time when the experiment was stopped (ca. 35 000 s).

the phase separation process, whereas the remaining domains are inhibiting and cooperate with the GFP part to induce the strongest effect observed in this series (see also the Supplementary discussion in the ESI†). These findings highlight that different domains in a protein can have fundamentally different impact on mineralisation, with the balance of competing and cooperating effects determining the net result.

Further interesting observations were made in the early post-nucleation stage (Fig. 3), where information on the nature of the formed phase can be inferred from the free ion products. In the reference experiment without any proteins, the nucleated particles have an apparent solubility of ca. $3.1 \times 10^{-8} \text{ M}^2$, which corresponds well with values reported for amorphous calcium carbonate (ACC) with calcitic short-range order in the literature.²⁹ The presence of GFP does not affect the average solubility product measured directly after nucleation (Fig. 3a), *i.e.* ACC is likely to be the initially formed



phase also in this case; however, the continued decrease in the free ion product observed between about 25 000 and 35 000 s (marked by red arrow in Fig. 3b) indicates the completed transformation of ACC into less soluble (and hence more stable) polymorphs; such effects were not observed for the reference over similar timescales (*i.e.* there was no measurable further decrease in the free ion product over a period of at least 10 000 s after the initial steep drop due to nucleation). This might imply that GFP accelerates the transformation process (relative to the reference without added proteins), or in other words, that it lowers the kinetic stability of ACC particles.

For the two fusion proteins, remarkably different behaviour can be discerned. Here, the free ion products detected after nucleation drop immediately to levels that are significantly lower than those expected for ACC in such experiments, namely 2.3×10^{-8} and $2.7 \times 10^{-8} \text{ M}^2$ for P1 and P2-3, respectively (*cf.* Fig. 3). This means either that a phase more stable than ACC is directly nucleated, or that ACC is extremely short-lived under these conditions and transforms rapidly into that more stable phase. Notably, the measured apparent solubilities are still considerably higher than literature values for crystalline polymorphs like vaterite ($1.2 \times 10^{-8} \text{ M}^2$) or calcite ($0.3 \times 10^{-8} \text{ M}^2$),³¹ the main products usually obtained from precipitation experiments at room temperature. However, X-ray diffraction (XRD) patterns of particles isolated at the end of the titration experiments clearly evidence that the only crystalline phase present in all samples at this stage is calcite (see Fig. S3 in the ESI†).

The controversial fact that higher apparent solubilities are detected in solution can have different reasons. First, it is well known that the amount of dissolved ions is determined by the most soluble phase occurring in the system and thus, mixtures of (X-ray amorphous) ACC and calcite will give the solubility of ACC as long as it exists in significant amounts.⁷ This is the case for the reference experiment without proteins, where scanning electron microscopy (SEM) images of the isolated solids (Fig. 4a) show micron-sized rhombohedral calcite crystals (black arrow) next to less defined networks of ACC nanoparticles (white arrow). By contrast, only well-developed calcite crystals (with different sizes) could be observed in the presence of all three proteins (Fig. 4b-d; note that the particles were extracted after the second decrease of the free ion product in the case of GFP). A second possible explanation for the higher apparent solubility of the crystals formed under the influence of the proteins relies on the size dependence of the thermodynamic stability of mineral phases like calcite:³² as particles become smaller, the larger surface-to-volume ratio decreases their overall stability (with calcite eventually being less stable than ACC for example)³³ and hence increases solubility relative to values reported for the corresponding bulk phases in the literature.³¹ However, the SEM images in Fig. 4 and additional TEM analyses (see Fig. S4 in the ESI†) strongly suggest that the crystals formed in the protein-containing experiments are much too large for such effects to become relevant. Finally, incorporation and/or

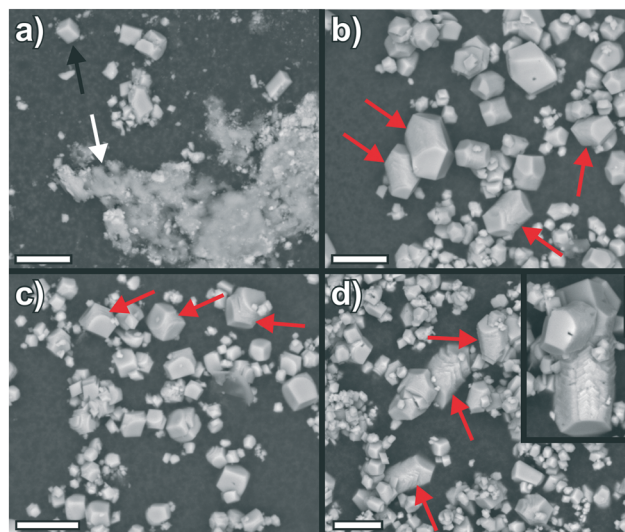


Fig. 4 SEM images of particles obtained from titration experiments a) in the absence of proteins, and in the presence of 0.01 mg mL⁻¹ of GFP, c) P1, and d) P2-3. Scale bars are 10 μm. Note that the particles were isolated at the time where the profiles of the free ion products in Fig. 3b stop (*i.e.* after about 10 000 s for the reference experiment and *ca.* 35 000 s for the protein-containing samples). In this way, the morphologies and phases observed by SEM are directly comparable to the apparent solubilities measured at the time of isolation.

occlusion of organic species into the crystal structure³⁴ can lead to a significant increase in solubility due to lattice distortions and consequent strains. This has been shown for single amino acids^{7,35} and is likely to apply for the three present proteins in a similar manner, as already demonstrated in a previous study;²⁵ such effects rationalise why relatively high solubility products are measured for both GFP alone and the two fusion proteins (Fig. 3) despite the obvious presence of large calcite crystals in the absence of significant amounts of ACC (Fig. 4). The strong interaction of the proteins with calcite also becomes manifest in the final morphologies of the crystals, which display distorted shapes as well as rounded edges and corners (instead of the usually observed sharp boundaries). This indicates (specific) adsorption of the proteins onto growing calcite faces, as confirmed by fluorescence microscopy imaging (see Fig. S5 in the ESI†) and reported previously for a number of other additives.^{7,36-38} In some cases, these effects are prominent and lead to elongation of the rhombohedra along their *c*-axis (highlighted by red arrows in Fig. 4b-d).

Concerning the early post-nucleation stage, our results thus show that both the full-length and the truncated GFP-perluciferin fusion proteins promote the formation of crystalline calcite (see also Fig. S4 in the ESI†), while GFP alone has a weaker effect and seems to mainly accelerate the ACC-to-calcite transformation. Although the full-length protein P1 leads to less soluble phases than the truncated variant P2-3, we cannot unambiguously argue which domain is responsible for the activating impact (see the Supplementary discussion in the ESI†). In any case, the observations made for



these perlucin derivatives are fundamentally distinct from the results of related studies on different CaCO₃ biomineralisation proteins such as SM50 (from the larval sea urchin spicule)¹³ or AP7 (from mollusk shell nacre).¹⁵ Apart from certain effects on ion association equilibria and greater or lesser nucleation inhibition, these proteins were found to either not modify the nature (and stability) of the formed CaCO₃ phase¹⁵ or to increase the apparent solubility product,¹³ possibly by stabilising liquid-like states analogous to the well-known polymer-induced liquid precursors (PILP).^{39–41} In another recent work,¹⁶ the N-terminal part of the framework matrix protein n16 from the pearl oyster *Pinctada fucata* was indeed proposed to favour the direct nucleation of vaterite over ACC formation; however, vaterite is not an integral component of the final biomineral and there was also no incorporation of protein into the crystals detected (as the measured solubility products were virtually identical with that of pure vaterite). In turn, the influence of perlucin derivatives on CaCO₃ crystallisation observed in the present experiments and in previous work²⁵ is commensurate with the supposed role of the native protein in nacre biomineralisation. Although we can only speculate about the particular mechanisms by which the proteins manage to favour the formation of crystalline CaCO₃ polymorphs over amorphous phases, they may do so by providing a structure that matches the respective crystal lattice, thus facilitating (templated) nucleation and allowing for specific protein-mineral interactions during growth (in line with the notion of protein incorporation into the inorganic structure).⁴² Thereby, the degree of intrinsic disorder of individual protein domains may play a major role in directing their particular mode of action in the biomineralisation process.⁴³

Conclusions

In this work, we have investigated the effect of recombinant perlucin derivatives on the crystallisation of calcium carbonate by using a potentiometric titration assay that permits detailed insights into pre- and early post-nucleation phenomena as well as the nucleation process itself. The collected data provide strong evidence that GFP-perlucin fusion proteins have an overall inhibiting influence on CaCO₃ nucleation and, most importantly, that they direct polymorph selection in favour of crystalline calcite, into which the proteins incorporate to a certain extent. Comparative experiments with full-length and truncated variants have furthermore shown that different domains in the protein can have distinct and sometimes opposing effects, so that the net impact is a balance of synergistic and competitive processes. Even though the used proteins were derivatives with an additional GFP moiety (which itself was found to interfere with nucleation and early growth), the observed *in vitro* behaviour helps to rationalise the role of perlucin in actual biomineralisation environments. Fine-tuning of nucleation kinetics and relative stabilities of different mineral phases at the onset of precipitation

might be a viable mechanism for controlling crystallisation processes *in vivo*.

While simplified model systems and well-defined crystallisation assays like those employed here can already substantially improve our understanding of the complex world of biomineralisation, it is obvious that further systematic studies are required to identify the individual contribution of different protein properties such as solubility, amino acid composition or conformation. In this context, artificial peptides and recombinant proteins may prove their value in the future for the design of potential “biomineralisation toolkits” enabling a greater level of control over mineral formation. In the end, the lessons learned from such studies may be applied to conceive advanced strategies for crystal engineering and material synthesis in general.

Acknowledgements

The authors thank A. Rao and J. K. Berg for help with some of the experiments. I. M. W. is grateful to E. Arzt for continuous support. E. W. thanks B. Pokroy for his support and helpful discussions.

Notes and references

- 1 S. Mann, *Biomineralization: Principles and Concepts in Bioinorganic Materials Chemistry*, Oxford University Press, Oxford, 2001; P. Behrens and E. Bäuerlein, *Handbook of Biomineralization*, Wiley-VCH, Weinheim, 2009.
- 2 S. Weiner and L. Addadi, *Annu. Rev. Mater. Res.*, 2011, **41**, 21.
- 3 B. Marie, C. Joubert, A. Tayale, I. Zanella-Cleon, C. Belliard, D. Piquemal, N. Cochennec-Laureau, F. Marin, Y. Gueguen and C. Montagnani, *Proc. Natl. Acad. Sci. U. S. A.*, 2012, **109**, 20986–20991.
- 4 J. L. Drake, T. Mass, L. Haramaty, E. Zelzion, D. Bhattacharya and P. G. Falkowski, *Proc. Natl. Acad. Sci. U. S. A.*, 2013, **110**, 7958–7959.
- 5 K. Gries, F. Heinemann, M. Gummich, A. Ziegler, A. Rosenauer and M. Fritz, *Cryst. Growth Des.*, 2011, **11**, 729–734.
- 6 M. Eder, M. Koch, C. Muth, A. Rutz and I. M. Weiss, *J. Struct. Biol.*, 2016, DOI: 10.1016/j.jsb.2016.03.015.
- 7 M. Kellermeier, H. Cölfen and D. Gebauer, *Methods Enzymol.*, 2013, **532**, 45–69.
- 8 D. Gebauer, H. Cölfen, A. Verch and M. Antonietti, *Adv. Mater.*, 2009, **21**, 435–439.
- 9 A. Picker, M. Kellermeier, J. Seto, D. Gebauer and H. Cölfen, *Z. Kristallogr.*, 2012, **227**, 744–757.
- 10 D. Gebauer, A. Verch, H. G. Börner and H. Cölfen, *Cryst. Growth Des.*, 2009, **9**, 2398–2403.
- 11 A. Rao, J. K. Berg, M. Kellermeier and D. Gebauer, *Eur. J. Mineral.*, 2014, **26**, 537–552.
- 12 A. Verch, D. Gebauer, M. Antonietti and H. Cölfen, *Phys. Chem. Chem. Phys.*, 2011, **13**, 16811–16820.



- 13 A. Rao, J. Seto, J. K. Berg, M. Scheffner and H. Cölfen, *J. Struct. Biol.*, 2013, **183**, 205–215.
- 14 I. Perovic, E. P. Chang, M. Lui, A. Rao, H. Cölfen and J. S. Evans, *Biochemistry*, 2014, **53**, 2739–2748.
- 15 I. Perovic, A. Verch, E. P. Chang, A. Rao, H. Cölfen, R. Kröger and J. S. Evans, *Biochemistry*, 2014, **53**, 7259–7268.
- 16 J. Seto, A. Picker, Y. Chen, A. Rao, J. S. Evans and H. Cölfen, *Cryst. Growth Des.*, 2014, **14**, 1501–1505.
- 17 E. P. Chang, I. Perovic, A. Rao, H. Cölfen and J. S. Evans, *Biochemistry*, 2016, **55**, 1024–1035.
- 18 E. P. Chang, T. Roncal-Herrero, T. Morgan, K. E. Dunn, A. Rao, J. A. M. R. Kunitake, S. Lui, M. Bilton, L. A. Estroff, R. Kröger, S. Johnson, H. Cölfen and J. S. Evans, *Biochemistry*, 2016, **55**, 2401–2410.
- 19 K. Mann, I. M. Weiss, S. Andre, H. J. Gabius and M. Fritz, *Eur. J. Biochem.*, 2000, **267**, 5257–5264.
- 20 I. M. Weiss, S. Kaufmann, K. Mann and M. Fritz, *Biochem. Biophys. Res. Commun.*, 2000, **267**, 17–21.
- 21 T. Dodenhof, M. Fritz, S. Kelm and F. Dietz, *Cloning and expression studies of nacre protein perlucin from greenlip abalone *Haliotis laevis**, The EMBL Nucleotide Sequence Database, accession FN6744451, NCBI website, 2010.
- 22 T. Dodenhof, F. Dietz, S. Franken, I. Grunwald and S. Kelm, *PLoS One*, 2014, **9**, e97126.
- 23 S. Blank, M. Arnoldi, S. Khoshnavaz, L. Treccani, M. Kuntz, K. Mann, G. Grathwohl and M. Fritz, *J. Microsc.*, 2003, **212**, 280–291.
- 24 N. Wang, Y. H. Lee and J. Lee, *Comp. Biochem. Physiol., Part B: Biochem. Mol. Biol.*, 2008, **149**, 354–361.
- 25 E. Weber, L. Bloch, C. Guth, A. N. Fitch, I. M. Weiss and B. Pokroy, *Chem. Mater.*, 2014, **26**, 4925–4932.
- 26 E. Weber, C. Guth, M. Eder, P. Bauer, E. Arzt and I. M. Weiss, *MRS Online Proc. Libr.*, 2012, **1465**, mrss12.
- 27 D. Blohm, J. Zeng, M. Fritz and G. Grathwohl (University of Bremen), *Pat. WO2007125127A2*, 2007.
- 28 E. Weber, C. Guth and I. M. Weiss, *PLoS One*, 2012, **7**, e56653.
- 29 D. Gebauer, A. Völkel and H. Cölfen, *Science*, 2008, **322**, 1819–1822.
- 30 D. Gebauer, M. Kellermeier, J. D. Gale, L. Bergström and H. Cölfen, *Chem. Soc. Rev.*, 2014, **43**, 2348–2371.
- 31 L. Brecevic and A. E. Nielsen, *J. Cryst. Growth*, 1989, **98**, 504–510.
- 32 T. Z. Forbes, A. V. Radha and A. Navrotsky, *Geochim. Cosmochim. Acta*, 2011, **75**, 7893–7905.
- 33 A. Navrotsky, *Proc. Natl. Acad. Sci. U. S. A.*, 2004, **101**, 12096–12101.
- 34 E. Weber and B. Pokroy, *CrystEngComm*, 2015, **17**, 5873–5883.
- 35 S. Borukhin, L. Bloch, T. Radlauer, A. H. Hill, A. N. Fitch and B. Pokroy, *Adv. Funct. Mater.*, 2012, **22**, 4216–4224.
- 36 D. B. De Oliveira and R. A. Laursen, *J. Am. Chem. Soc.*, 1997, **119**, 10627–10631.
- 37 C. A. Orme, A. Noy, A. Wierzbicki, M. T. McBride, M. Grantham, H. H. Teng, P. M. Dove and J. J. De Yoreo, *Nature*, 2001, **411**, 775–779.
- 38 M. Kellermeier, E. Melero-Garcia, W. Kunz and J. M. Garcia-Ruiz, *Adv. Chem. Phys.*, 2012, **151**, 277–307.
- 39 M. A. Bewernitz, D. Gebauer, J. Long, H. Cölfen and L. B. Gower, *Faraday Discuss.*, 2012, **159**, 291–312.
- 40 S. E. Wolf, J. Leiterer, V. Pipich, R. Barrea, F. Emmerling and W. Tremel, *J. Am. Chem. Soc.*, 2011, **133**, 12642–12649.
- 41 J. S. Evans, *CrystEngComm*, 2013, **15**, 8388–8394.
- 42 M. Suzuki, K. Saruwatari, T. Kogure, Y. Yamamoto, T. Nishimura, T. Kato and H. Nagasawa, *Science*, 2009, **325**, 1388–1390.
- 43 J. S. Evans, *Bioinformatics*, 2012, **28**, 3182–3185.

